2014

Feasibility study of a two-fluid small modular molten salt reactor with in core heat removal capability

Brandon James Lahmann

Department:

FEASIBILITY STUDY OF A TWO-FLUID SMALL MODULAR MOLTEN SALT REACTOR WITH IN CORE HEAT REMOVAL CAPABILITY

by

BRANDON JAMES LAHMANN

A THESIS

Presented to the Faculty of the Graduate School of the

MISSOURI UNIVERSITY OF SCIENCE AND TECHNOLOGY

In Partial Fulfillment of the Requirements for the Degree

MASTER OF SCIENCE IN NUCLEAR ENGINEERING

2014

Approved by

Ayodeji Alajo, Advisor
Shoaib Usman
Carlos Castaño

ABSTRACT

A feasibility study of a two-fluid small modular molten salt reactor (MSR) with in core heat removal was performed. The initial fuel block dimension for the configuration was based on the Fuji MSR. The fuel was a mixed fluoride salt of density 3.25 g/cc, composed of 71 LiF – 16 BeF_2 – 12 ThF_4 – 1 $^{233}UF_4$ molar percentages. The coolant salt was Li_2BeF_4 (FLiBe) of density 1.94 g/cc. The work set out to establish whether or not such a reactor is thermodynamically feasible when optimized for various neutronics parameters. A Java based API was developed to facilitate the neutronics optimization of the reactor concept.

In the simulation studies that followed (performed in MCNP), it was established that the optimal block dimension and fuel volume fraction to support under-moderation requirements are 20 cm across flats and 0.15 respectively. Fuel channel diameters varied from 12 cm to 9 cm such that neutron leakage could be suppressed while maintaining a radial power peaking factor of 2.20. In all the simulations except for temperature reactivity calculations, the reactor was assumed isothermal at 900 K. The average temperature coefficient of reactivity was calculated as -5.87E-5 $\Delta k/k$-K.

Thermo hydraulic studies performed in STAR CCM+ revealed that complete in core heat removal cannot practically be achieved in a design purely optimized for neutronics. However, it was found that fractional heat removal ranging from 15% - 85% can be achieved with sufficient mass flow rates. Potential improvements necessary for complete in core heat removal are theorized and briefly discussed.

ACKNOWLEDGMENTS

I would like to give my sincerest thanks to Dr. Shoaib Usman, my original research advisor and member of my thesis committee, for seeing the potential in me very early in my academic life and for first introducing me to the path of research and discovery. Before meeting with Dr. Usman as a sophomore, I had no serious intentions on continuing my educational career further than my undergraduate degree. Had it not been for his early recommendations, none of this would have been possible. Dr. Usman made an enormous leap of faith that day in allowing a sophomore he had just met to do research under him and for that I will be eternally grateful.

I would also like to thank Dr. Ayodeji Alajo, my current research advisor and my thesis committee chair for having always been extremely kind and encouraging in the short time we have known each other. Dr. Alajo has never hesitated to immediately make time for me as needed throughout the course of my work and has never failed to point me in the right direction during times of difficulty. Dr. Alajo has always displayed an immense amount of trust in me evident by the great freedom and flexibility he has always offered me. For these reasons and more, Dr. Alajo is by far the best advisor and mentor I could have ever hoped to ask for.

I am extremely appreciative of Susan Sipaun for bringing STAR CCM+ to my attention early in my work and for helping me understand the software as I was learning it. Much of this work would not have been possible without her patience and generosity.

Last but not least, I'd like to thank my parents, Theresa and Andrew Ninichuck, for their loving support and encouragement throughout my life. I owe much of my success to my parents for constantly being able to see the potential in me when I could not.

TABLE OF CONTENTS

LIST OF ILLUSTRATIONS

LIST OF TABLES

1. INTRODUCTION

Molten salt reactors (MSRs) are one of the most promising of the Generation IV reactors currently being explored and developed today. They are unique in the fact that they make use of a molten salt primary coolant which will often additionally serve as the reactor's fissionable material. These fluid fuel designs lend themselves to several inherent passive safety features not available to conventional solid fueled reactors, making the MSR concept appealing in a post-Fukushima society. Furthermore, MSRs are also capable of high operating temperatures which ensure high thermal efficiencies, operation at atmospheric pressures which greatly simplifies designs, and operating with minimal excess reactivity thanks to the active removal of fuel poisons during operations [1].

In a standard liquid fueled MSR design, the fuel salt acts both as the fissionable material and the primary coolant. This generally means that the removal of heat from the fuel will take place in some external intermediate heat exchanger and not directly at the location of heat generation [1]. This fact makes it such that the fuel salt will raise and lower in temperature as it is transported throughout the system. This steady state process of the fuel losing and gaining temperature is antithetical to conventional solid fueled reactors where the heat removal takes place directly in the core. Ultimately, this means that the average temperature of the fuel will be less than what would otherwise be achievable in a system where the fuel temperature could be relatively constant throughout. These lower than ideal average temperatures increases the required mass flow rate through the external heat exchanger needed to adequately remove heat from the fuel.

MSRs have much to gain from minimizing the mass flow rate of the fuel salt. Many of the appealing advantages of the liquid fueled MSR concept revolve around the ability to

chemically process the fuel as the reactor is at power. Beyond the obvious advantages of efficiency and stability, slower fuel velocities will help simplify these chemical processing systems, making features like online refueling and active poison removal easier to implement. As such, designing a MSR in such a way that the heat removal will take place at the location of heat generation could prove favorable if it would result in lower mass flow rates.

This thesis will develop and consider a MSR design that introduces a secondary fluid in the core to act as the fuel's primary coolant. In this way, the design will act much like a conventional solid fueled reactor design where the fuel's heat is generated and removed within the core, whilst still preserving the many attractive inherit safety features attributed to liquid fuels. In addition, the enclosed design was also subject to the criteria of a small modular reactor. The final product will be made such that the entire primary system can be contained within a 3.5 meter diameter making off-site construction possible. To further emphasize this purpose, the MSR was designed to have a modest thermal output of 75 MW.

2. NEUTRONICS MODELING AND OPTIMIZATION FRAMEWORK

Neutronics modeling was handled entirely by the Monte Carlo simulator MCNP5 and MCNPX 2.70. In addition, an API was developed in Java to help automate the process of geometry optimization. The API is designed to move the geometry building process from the conventional MCNP input decks to a more flexible Java environment. This takes advantage of the object oriented nature of Java programming by equating MCNP cells, surfaces, tallies, materials, and decks to Java Objects. This generalization of the process allows the user to focus more on the geometry itself while allowing the API to handle the stringent formatting requirements of MCNP. Being a Java API, users have full access to standard Java libraries and basic features expected of any programming language. Specifically, this allows the user to create simple scripts to automate the creation, running, and parsing of MCNP jobs.

MCNP models varied significantly between the various studies discussed in the following section and will be described in context of their respective studies. Despite this, all models shared a collection of common features listed below:

- All models are isothermal at a temperature of 900K. Cross sections used are from ENDF-7 evaluated at 900K unless otherwise stated
- Fuel material was modeled as a 71 LiF – 16 BeF_2 – 12 ThF_4 – 1 $^{233}UF_4$ (by molar percent) salt mixture of density 3.25 g/cc [2] [3]
- Coolant material was modeled as a Li_2BeF_4 (FLiBe) salt of density 1.94 g/cc [4]
- Moderator material was modeled as graphite of density 1.82 g/cc using the S(α,β) data set provided by MCNP [5]

3. NEUTRONICS DESIGN AND FEASIBILITY STUDIES

3.1 INITIAL FUEL CHANNEL DIMENSION OPTIMIZATION

Traditional fluid fueled MSR designs can feature a lattice of hexagonal graphite assemblies with a hollowed out fuel channel in the center [6] [7]. A basic cross sectional of this geometry is depicted in Figure 3.1. The first study will solely consider this most basic component and attempt to optimize its dimensions for the final design. To do this, an infinite lattice of these assemblies was modeled in MCNP5 using reflective conditions on all the boundaries. In an infinite configuration, the only variable dimensions are the size of the fuel channel and its spacing from adjacent channels (which is equivalent to the flat to flat distance of the hexagon). As a starting point, a flat to flat distance of 20 cm was considered based on the MSR Fuji, which is a similar reactor design [3]. The fuel channel size was then varied in the infinite configuration and plotted with its resultant eigenvalues. The results of this study are shown in Figure 3.2.

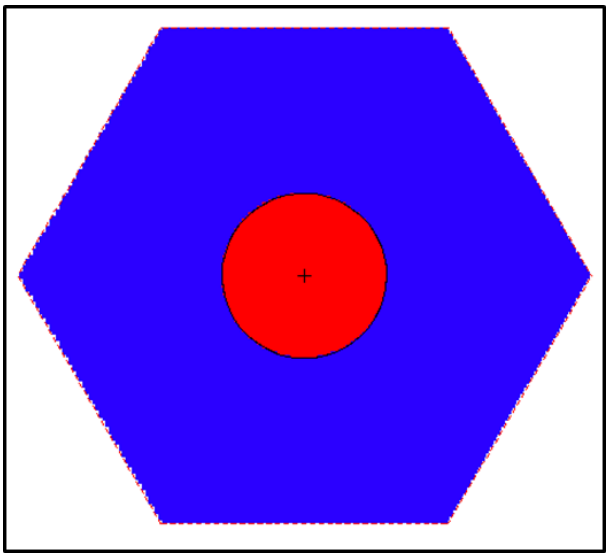

Figure 3.1. Cross Section of Basic MSR Fuel Channel

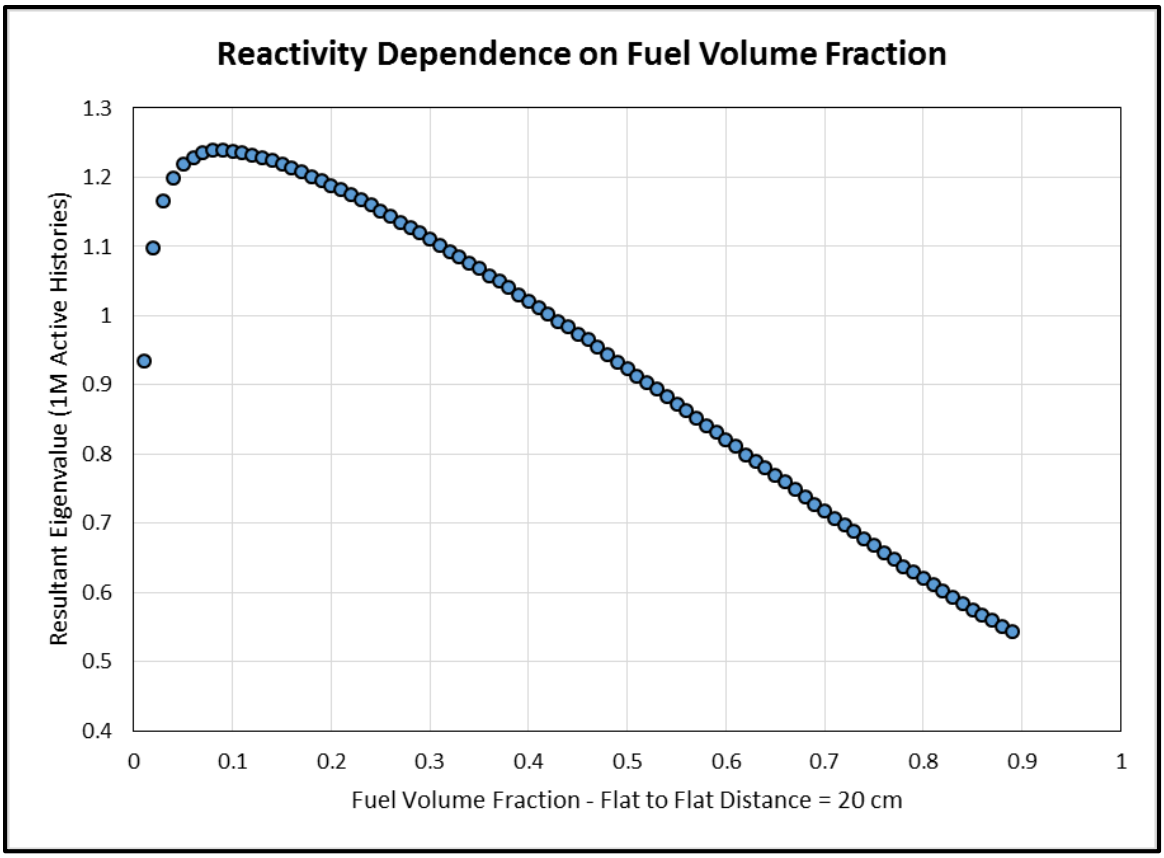

Figure 3.2. Resultant Eigenvalues of Varying Fuel Volume Fractions

The maximum eigenvalue occurs with a fuel volume fraction of approximately 10%, making it the optimal size for the design. It should be noted that other sizes will have to be used later in the design for power flattening since fuel enrichments cannot be varied in a liquid fuel reactor. To further verify this configuration, another series of simulations were performed with varying flat to flat distances. In this study, the fuel volume fraction was maintained at a constant 10% because of the results of the previous study. As before, the resultant eigenvalues were plotted with their respective flat to flat distances. The results of this study are shown in Figure 3.3.

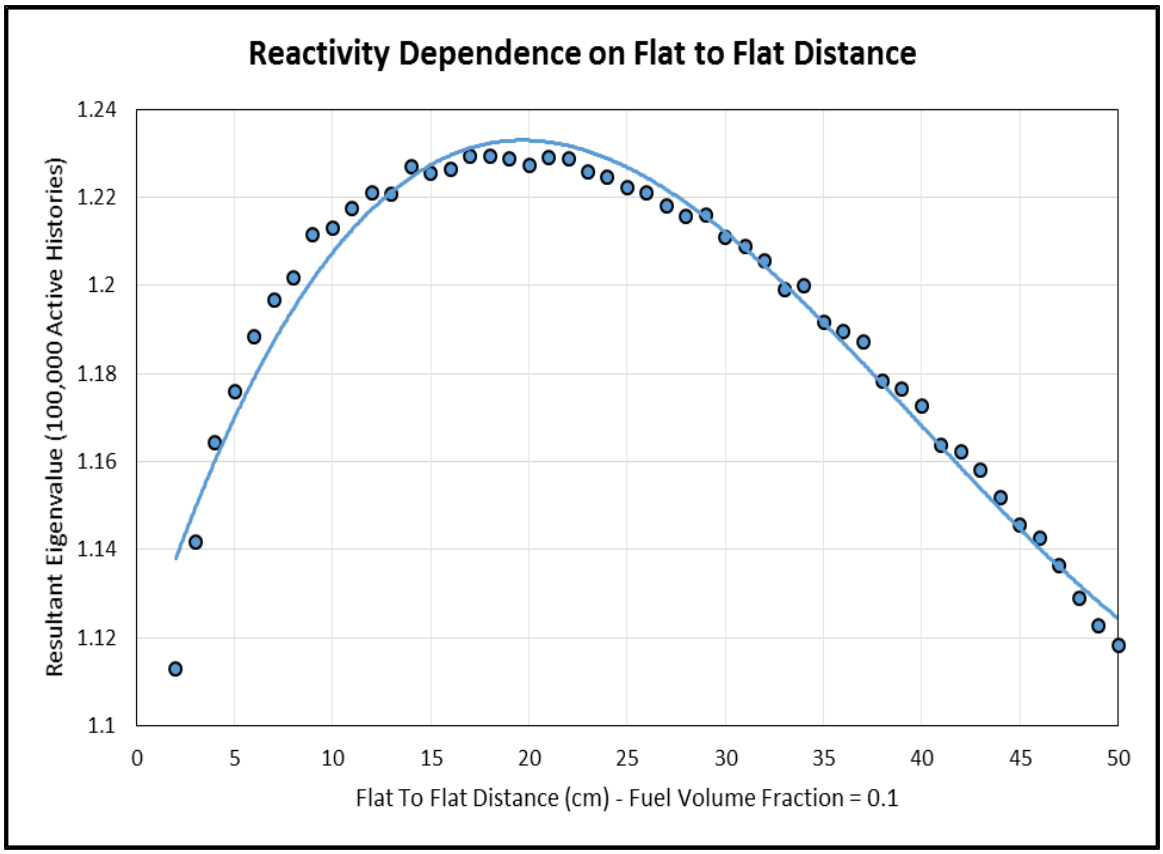

Figure 3.3. Resultant Eigenvalues of Varying Flat to Flat Distances

The maximum eigenvalue occurs with a flat to flat distance of near 20 cm. This verifies the initial choice and sets the size of all fuel channels to be used in the reactor core. It is important to note that we have only inspected two projections of potential size variations. For true completeness, all combinations of fuel volume fractions and flat to flat distances would need to be inspected. However, this is impractical and would likely result in the exact same conclusions. From a safety standpoint, a local maximum in reactivity is sufficient assuming reactor dimensions will not dramatically change during operations. Furthermore, the flat to flat distance of the channels will be difficult to change even in the worst accident scenarios. Therefore, it is concluded that the optimal channel size for the reactor will have a flat to flat distance of 20 cm with a fuel volume fraction of approximately 10%.

3.2 COOLANT CHANNEL CONSIDERATIONS

The two-fluid reactor must also allow for coolant channels to flow through the core to ensure the removal of heat generated within. It is proposed that smaller coolant channels be incorporated into every fuel channel instead of using two separate channels throughout the core. An example of the proposed design is shown in Figure 3.4. The coolant salt will be Li_2BeF_4 (FLiBe) which was chosen for its favorable moderator properties and chemical compatibility with the fuel salt. It is noted though, that graphite is a better moderator so inclusion of the coolant is expected to have negative effects of reactivity. The question becomes how big this effect will be, and what, if any, size limits will need to be imposed on the coolant channels. To test this, a moderately sized reactor (6 fuel channel rows with a 50 cm thick graphite reflector) was designed using the optimal fuel channel sizes discovered in the previous two studies. Coolant channels were included in the fuel channel assemblies using the proposed design depicted in Figure 3.4, and coolant channel sizes were varied. The effect of these size variations on the eigenvalue is shown plotted in Figure 3.5.

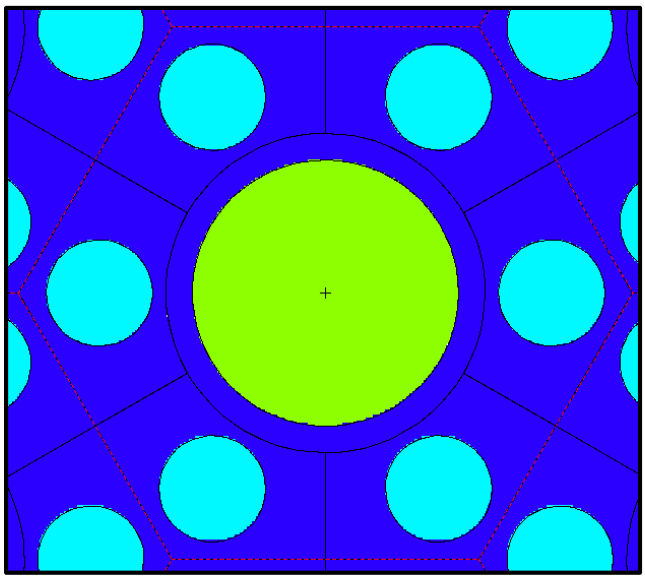

Figure 3.4. Cross Section of Proposed Two Fluid Fuel Channel Assembly

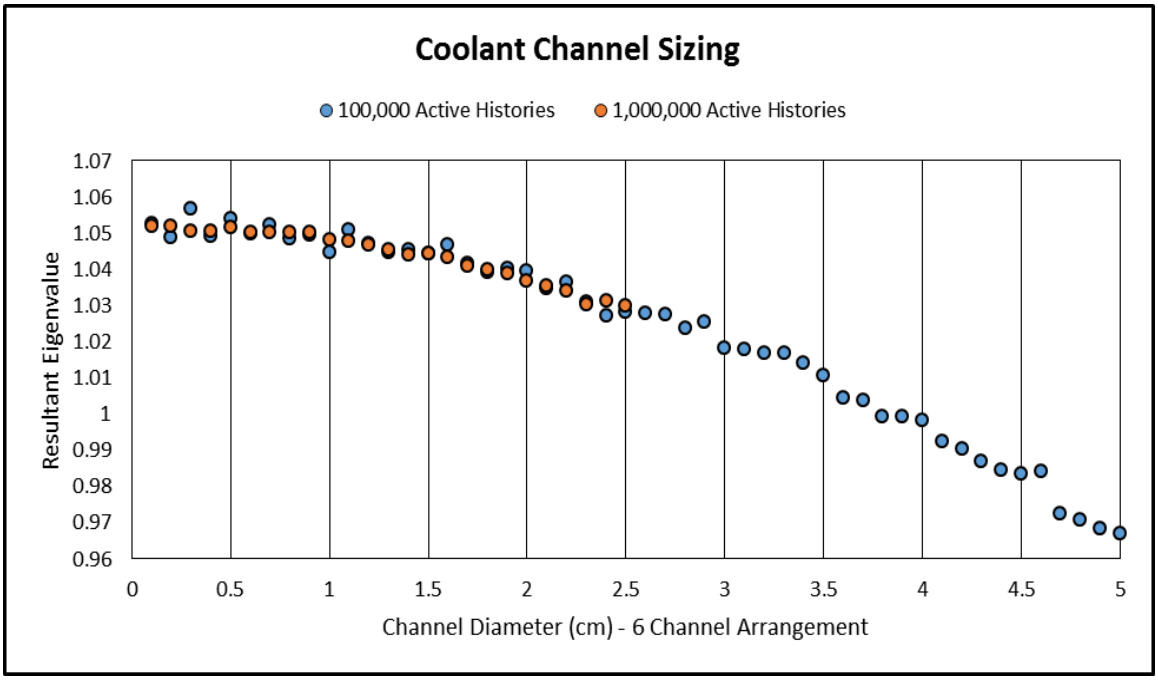

Figure 3.5. Resultant Eigenvalues of Varying Coolant Channel Sizes

As expected, when the coolant channel size increases reactivity is lost. The rate of reactivity loss appears to be proportional to the square of the diameter (proportional to the area) of the coolant channel. Ultimately, the size of the coolant channel will be determined by thermo-hydraulic concerns but this study offers insight on potential neutronics limitations. The next concern was the effect that the coolant channel's proximity to the fuel channel might have on reactivity. To study this, an arbitrary coolant channel size (2 cm diameter) was used and placed at various distances from the fuel channel in a configuration similar to the one shown in Figure 3.4. The resultant eigenvalues of these varying distances are shown plotted in Figure 3.6.

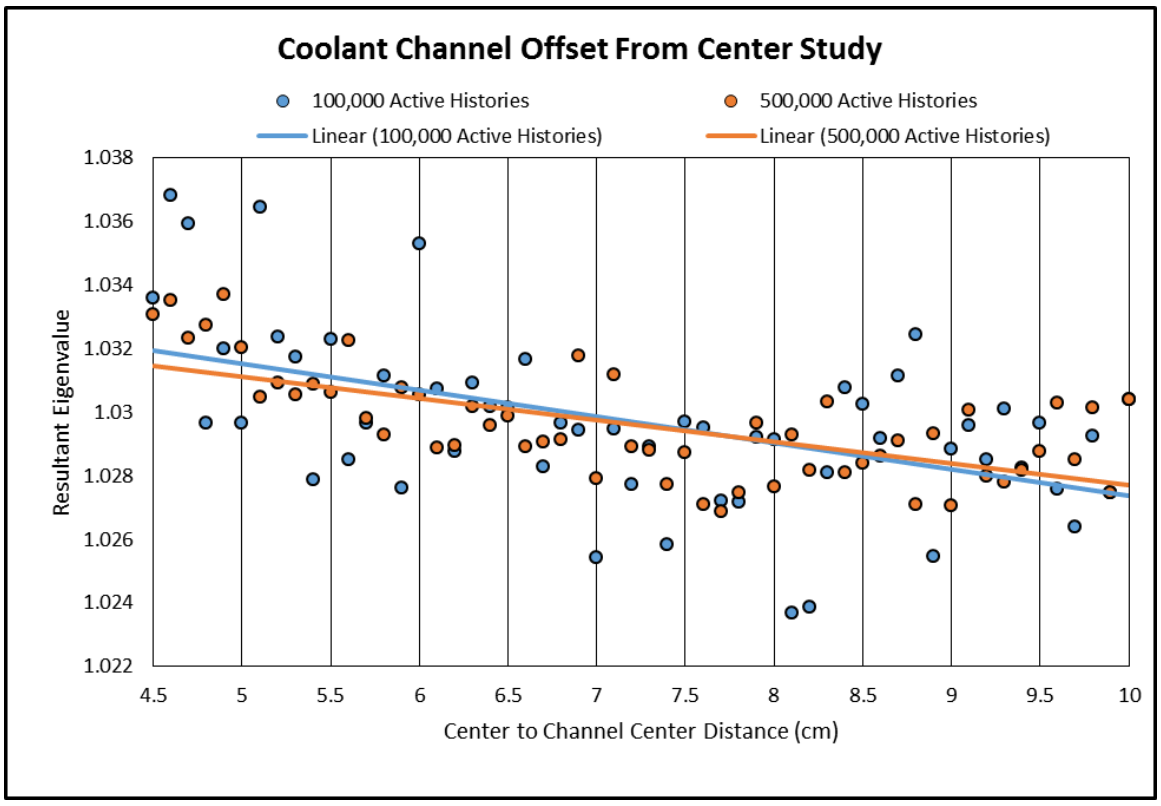

Figure 3.6. Resultant Eigenvalues of Varying Coolant Channel Spacing

The effect of the coolant channel's proximity to the fuel channel on reactivity is not big enough to overcome the stochastic noise of MCNP. Even using a linear fit shows that the effect is likely minor, although in favor of closer channels. However, because the effect is thought to be inconsequential, the coolant channels will be placed at a maximum distance to ensure increased flexibility when varying fuel channel sizes in future studies. Additionally this should benefit the structural reliability of the graphite by increasing the thickness between channels. At a maximum distance, the coolant channels center is located at the edge of the hexagon. In this way, a fuel channel only truly contains 2 (6 1/3 segments) coolant channels. This will benefit the neutronics of the core by reducing the overall flow area of coolant in the core. Additionally, manufacturing of the graphite channels is expected to be easier this way since the shape can be predefined by a mold rather than drilling multiple holes

into each channel. Again, the final size of the coolant channel must be determined by thermo-hydraulic studies and will be arbitrarily set to a diameter of 4 cm until such studies are performed. A depiction of this design is shown in Figure 3.7.

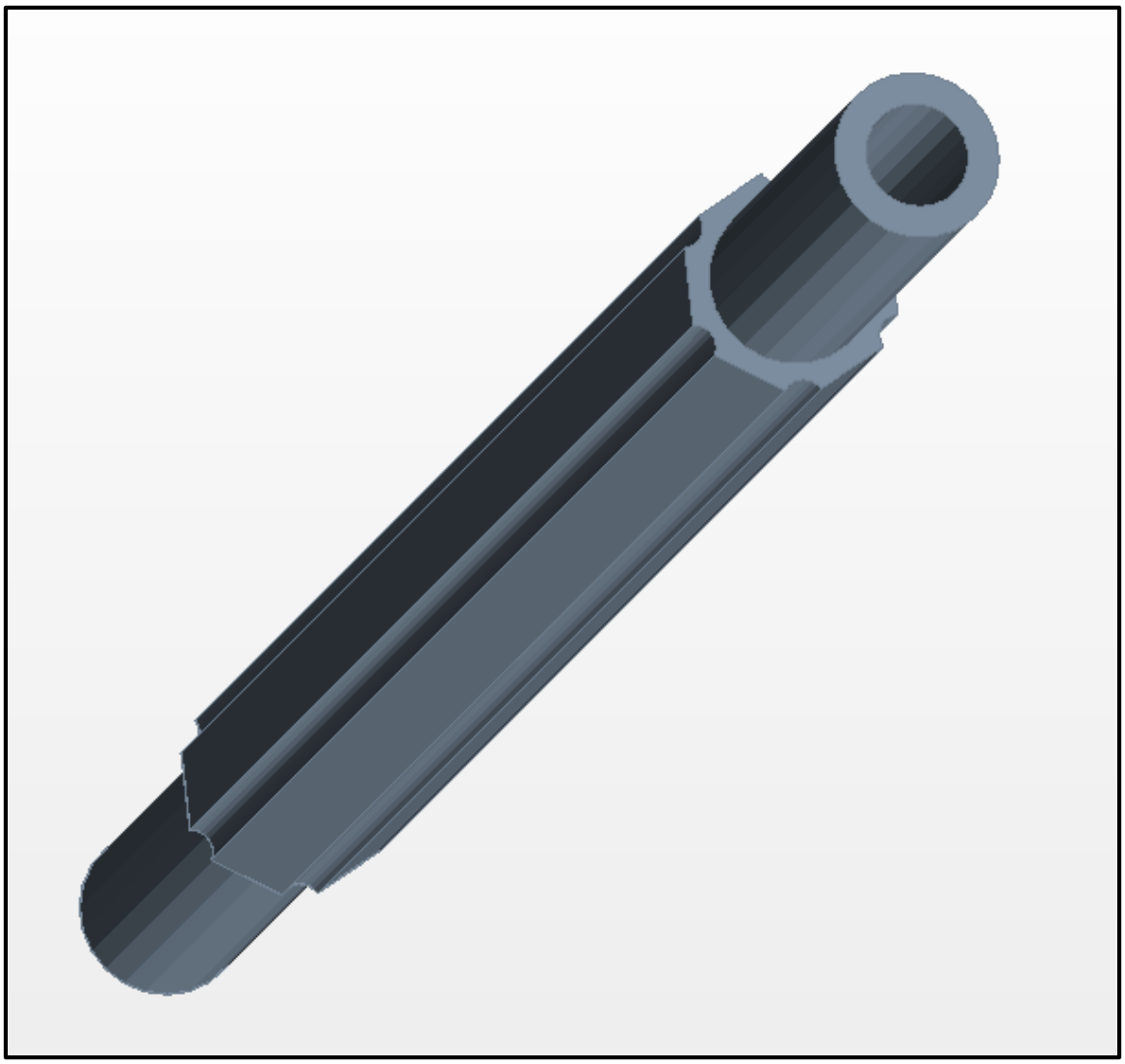

Figure 3.7. Two Fluid Fuel Channel Assembly with Coolant Channel Edges

3.3 REFINED FUEL VOLUME FRACTION STUDY

With the geometry of the coolant channels determined, it was thought that a re-optimization of the fuel channel size would be necessary. The inclusion of coolant reduces the net moderation and thus may impact the optimal fuel channel size. To investigate this concern, the optimization study performed in Section 3.1 was repeated using a finite geometry. This study featured six rows of channels using the fuel block design shown in Figure 3.7. Additionally, the core featured a 50 cm thick graphite radial and axial reflector which surrounded the fuel lattice. Finally, the core height was set at 2.5 m to match (twice) the core radius. The results of this study are shown plotted in Figure 3.8. Note that the optimal fuel volume fraction appears to be 15% in this study (previously 10%) but the reactivity appears to be mostly unaffected between 10% and 20%.

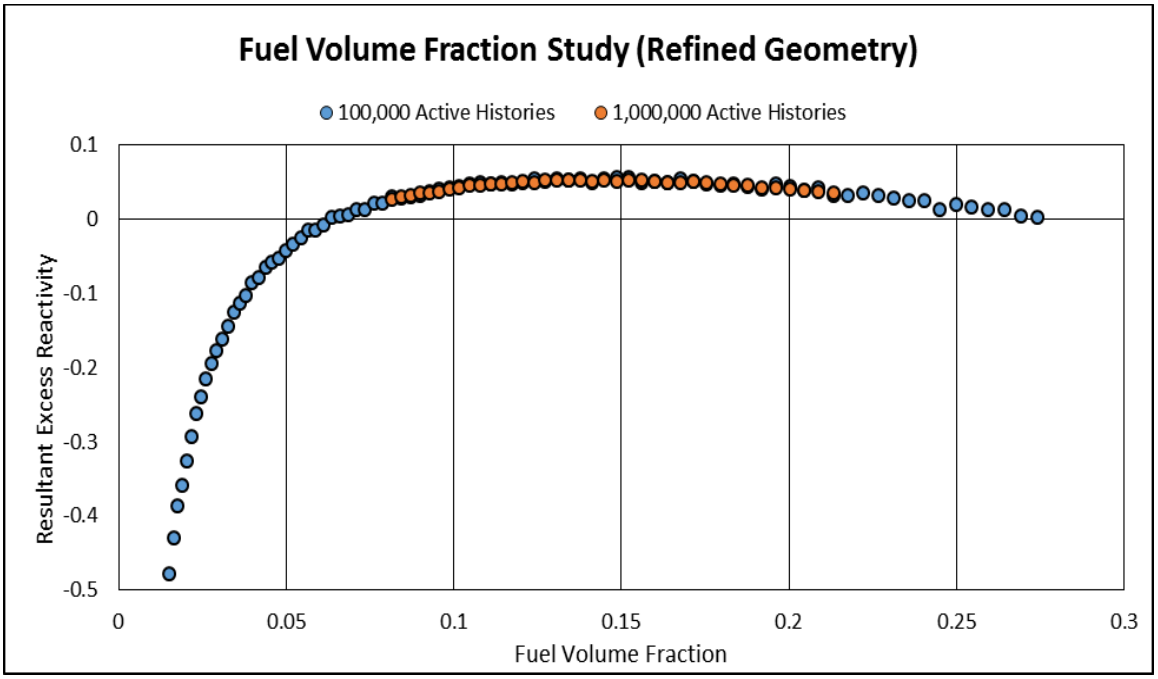

Figure 3.8. Reactivity of Varying Fuel Volume Fraction with Refined Geometry

3.4 POWER FLATTENING STUDIES

Flattening a reactor's power profile is extremely desirable for any reactor design. Doing so reduces the requirements on the coolant systems by decreasing the requirements in the hottest channel. Additionally, it leads to increase in total power since the coolant system is generally designed for the hottest channel. In conventional solid fueled reactors, the flattening of the power profile is often accomplished by varying the fuel enrichment throughout the core. Unfortunately, this practice is not possible in a liquid fueled MSR since the fuel fluid is constantly flowing and mixing throughout the system. Instead, power profiles can be flattened by varying the sizes of the fuel channels throughout the core. By using less optimal fuel volume fractions in areas where flux would be expected to be high, one can effectively lower the local value. It should be noted that this solution can only be used to flatten fluxes in the radial direction. Using axial-varying channel sizes (while not impossible) will be considered impractical for the purpose of this study and thus will not be considered.

In order to determine the optimal combination of fuel channel sizes, scripts from the developed Java API were used to vary the sizes of fuel channel by individual rows. For example, a script might vary the sizes of all the fuel channels in row 1 while maintaining the sizes of all other fuel channels. Studies were performed subsequently, starting from the center, such that the optimal size from a previous study would be used in the next. The effectiveness of a given configuration was determined by its power peaking factor as calculated by the Java API. This factor was calculated using the following equation:

$$F_{xy} \approx \frac{N_P \cdot P_{max}}{\sum_i \sum_j \overline{P_{ij}}} \quad \textbf{(1)}$$

Where F_{xy} is the power peaking factor, N_P is the number meshes that resolved a non-zero local power, and P_{ij} is the local averaged power in mesh element ij. It should be noted that the result of this equation is an approximation of the true value. Using "finite" meshes will unavoidably result in meshes that contain both fueled and non-fueled regions. These meshes will produce deceptively low local powers by averaging over the volume of the entire mesh. Ultimately, this results in a higher power peaking factor by lowering the average power. This effect can only be combatted by using finer meshing, approaching the true value as the number of meshes approach infinity. The results of these studies are shown plotted in the Figure 3.9. Additionally, the resultant optimal sizes are listed in Table 3.1 and the resultant power profile is shown in Figure 3.10.

Table 3.1. Optimal Power Peaking Fuel Channel Sizes

Row Number	**Optimum Diameter (cm)**
0	12.0
1	12.0
2	12.0
3	10.0
4	10.0
5	9.0
6	9.0

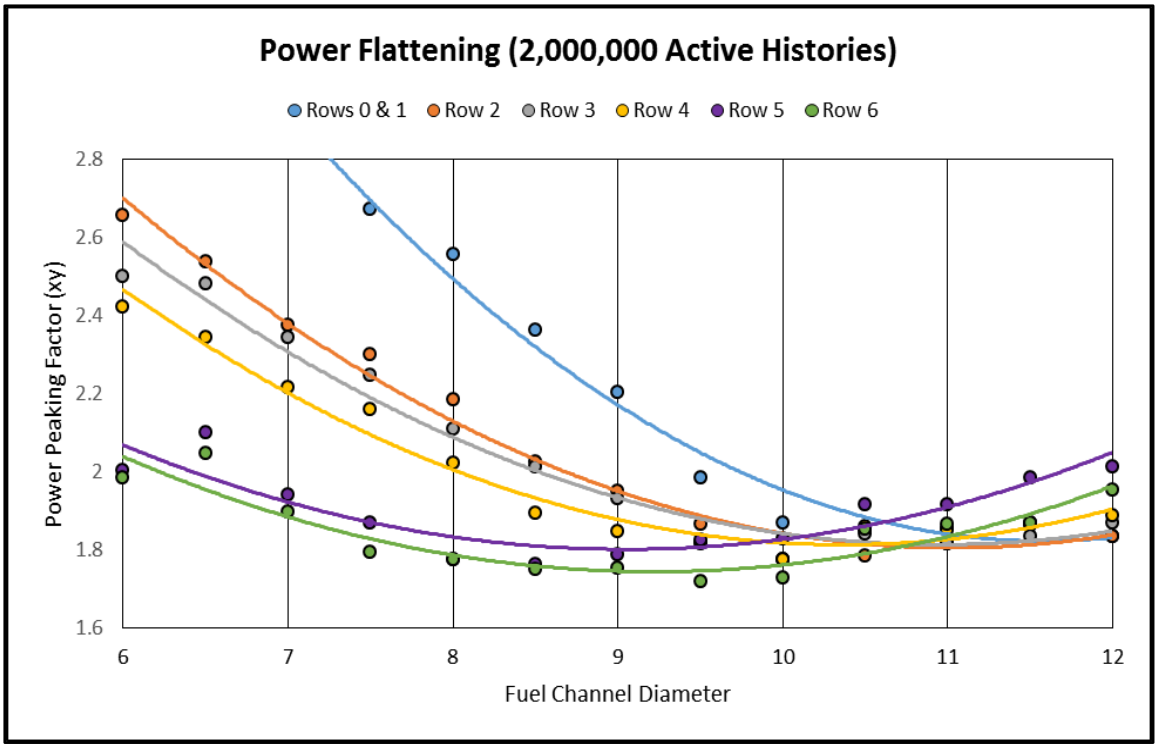

Figure 3.9. Power Peaking Factor of Varying Fuel Channel Sizes

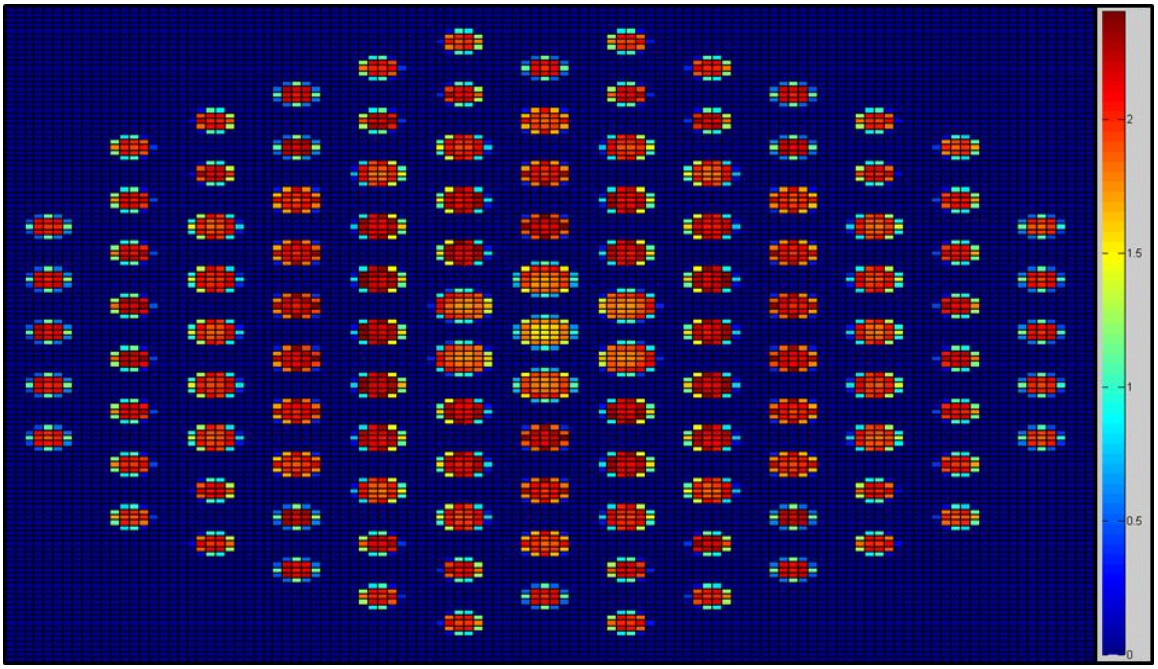

Figure 3.10. Resultant "Optimal" Power Profile (Arbitrary Units)

Interestingly, in the “optimal” configuration the biggest deviation from the average power occurs at the center of core where the lowest power density apparently exists. This is likely a result of the center channel carrying little weight in the power peaking factor calculation, making its contribution more susceptible to stochastic noise. Additionally, it may be the case that the numerous "boundary” meshes lower the apparent average power such that a drop in power will deceptively lower the power peaking factor. Regardless, this configuration is an excellent start and can be corrected manually or with improved meshing of the reactor model.

3.5 NEUTRON LEAKAGE STUDIES

Despite the relatively flat profile seen in Figure 3.10, the reactor does little to prevent leakage. By disregarding leakage, the reactor’s neutron economy will not be as efficient as it could be, resulting in a reactor that is larger than necessary. Additionally, high leakage will result in increased shielding requirements due to the increase of neutrons escaping the core. To test what effect preventing leakage would have on the reactivity of the core, a smaller 5-row MCNP model was constructed and tested using three different configurations. The first of the three was essentially the same model whose power profile is shown in Figure 3.10 but with one less row of fuel channels. The second, used a one row thick “blanket” that consisted of under-moderated fuel channels to reduce leakage. The third was simply an extension of this idea using a two row thick blanket instead. Cross sectional core diagrams of all three configurations are provided in Figure 3.11. Additionally, some important neutronics characteristics of each are summarized in Table 3.2.

Table 3.2. Neutronics Characteristics of Various Core Configurations

Reactor Configuration	Final Eigenvalue	Non-Leakage Probability	Power Peaking Factor
0 Row Blanket	0.99493	0.836	1.71
1 Row Blanket	1.01836	0.840	2.20
2 Row Blanket	1.00383	0.847	2.45

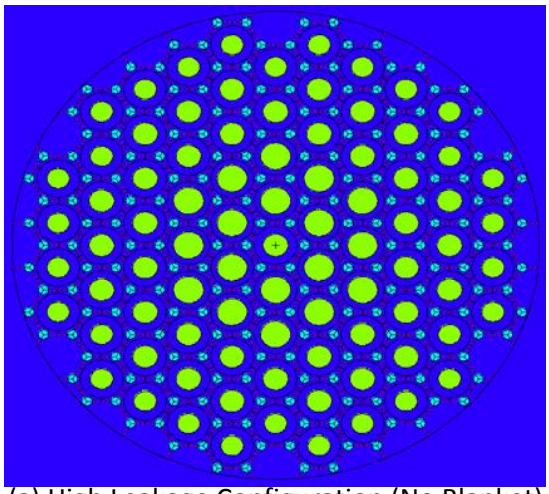

(a) High Leakage Configuration (No Blanket)

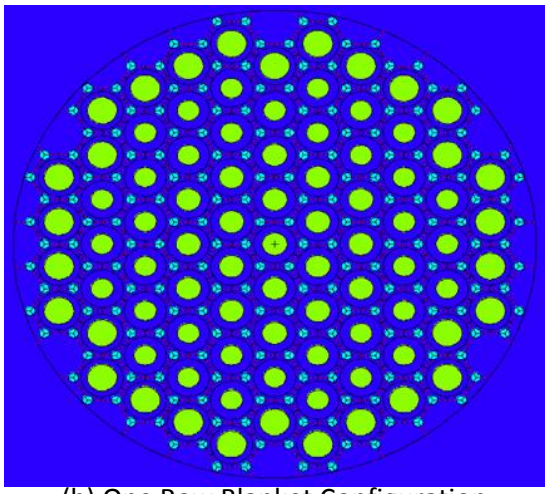

(b) One Row Blanket Configuration

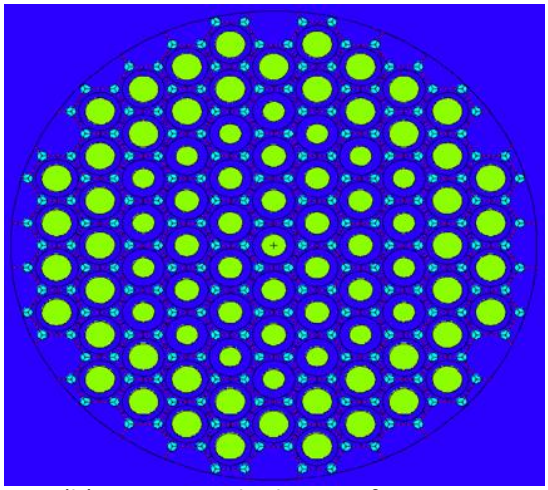

(b) Two Row Blanket Configuration

Figure 3.11. Cross Section of Core Configurations Used in Leakage Studies

Table 3.2 shows that the previous flat power profile configuration cannot be made critical when the reactor size is reduced to five rows. By adding a blanket of oversized (under moderated) channels to the peripheral, the necessary size of the reactor can be reduced. Obviously, this comes at the cost of increasing the power peaking factor since the blanket channels will drastically reduce local power due to under moderation. However, the decrease in size and more efficient use of neutrons is considered to be more desirable than the loss in power peaking optimization. Observe also, that using a two row thick blanket results in a loss of reactivity despite the increase in the non-leakage probability. At this point, the reactivity loss due to under moderation will outweigh reactivity gains due to the prevention of leakage. For this reason, a simple one row thick blanket displayed in Figure 3.11(b) will be optimal. For completeness: the resultant power profile, thermal flux profile, and fast flux profile of this configuration is shown in Figures 13.12, 13.13, and 13.14 respectively. Note that although all the units are arbitrary, the thermal and fast flux profiles are consistent with each other.

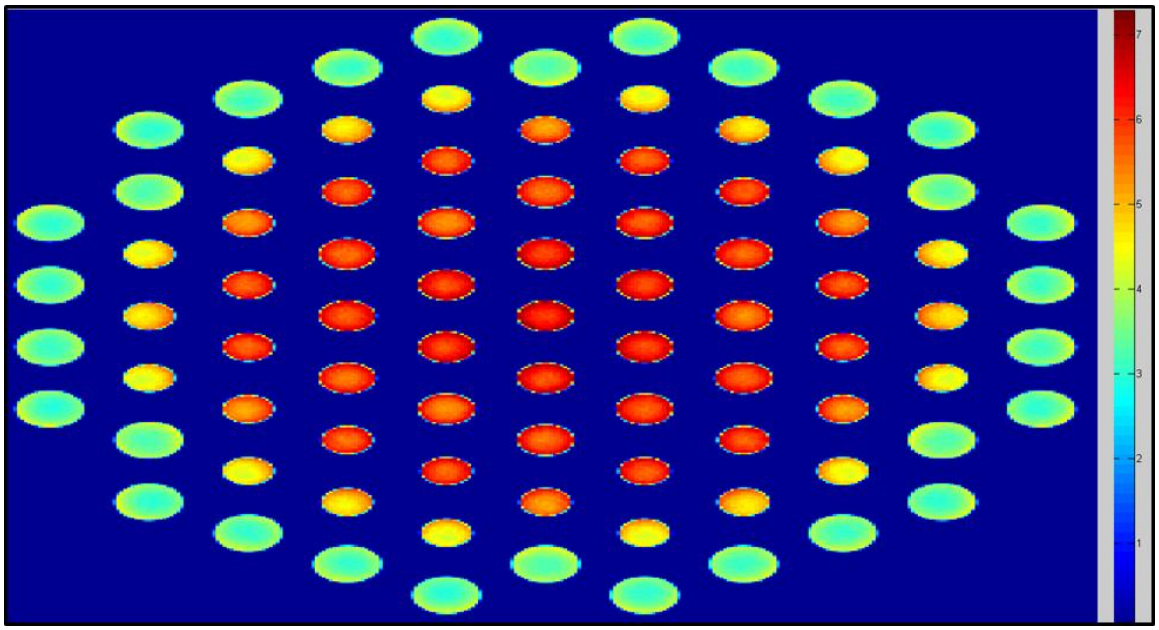

Figure 3.12. Power Profile of Final Core Configuration

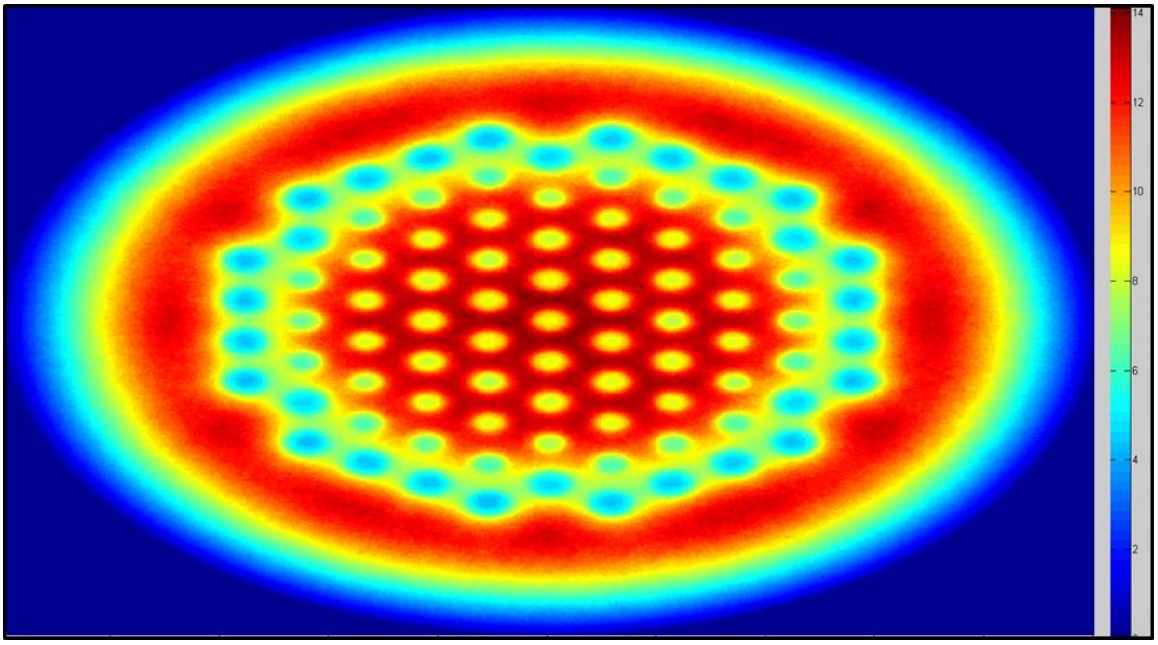

Figure 3.13. Thermal Flux Profile of Final Core Configuration

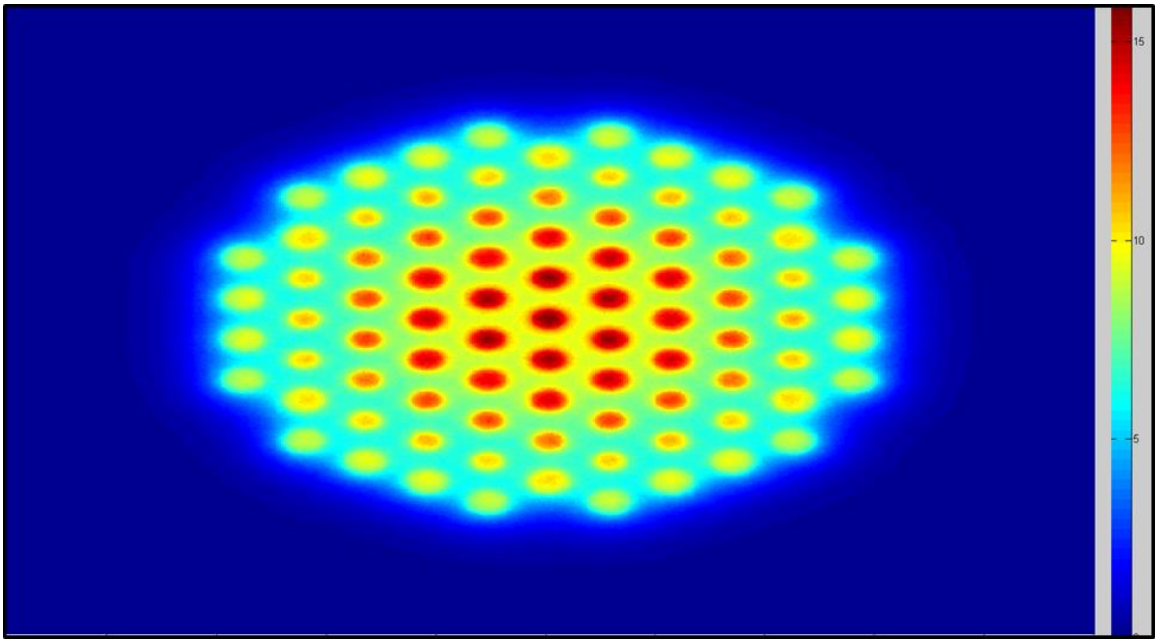

Figure 3.14. Fast Flux Profile of Final Core Configuration

3.6 REACTIVITY CONTROL SYSTEMS

For a complete design, the reactor requires a reactivity control system that can ensure adequate shutdown during any operational conditions. The reactor will utilize hastelloy cladded boron carbide rods as traditionally done in MSRs [8]. To ensure adequate shutdown with the one rod stuck condition, the reactor requires a total of four rods. The rods are to be placed in fuel channels as shown in Figure 3.15. The rods used in all studies have an arbitrary clad thickness of 1 cm and an arbitrary channel clearance of 1 cm. Both these dimensions need formal verification, but are thought to be conservative. Any decreases in either will increase the amount of poison in the rods and in turn increase all shutdown margins. Various shutdown margins using this configuration are shown in Table 3.3. The reactor will not feature any form of regulating rod for fine reactivity control. Instead the reactor will be self-regulated by the negative temperature coefficient of the fuel. Simulations showed that the average temperature reactivity coefficient of the fuel is -5.87E-03 % Δk/k-K. In the reactor's final configuration, this allows the fuel to reach average temperatures of approximately 980 K before criticality can no longer be sustained. Additionally, this offers an alternative means of reactivity control via the cooling system. Reactor power can be changed by throttling or increasing coolant flow rates into the core.

Table 3.3. Final Configuration Shutdown Margins

Parameter	**Absolute Reactivity Worth (% Δk/k)**
Shutdown Margin (Hot Core)	8.342362
Shutdown Margin – 1 Stuck Rod (Hot Core)	5.773096
Shutdown Margin (Cold Core)	4.601416
Shutdown Margin – 1 Stuck Rod (Cold Core)	2.123140

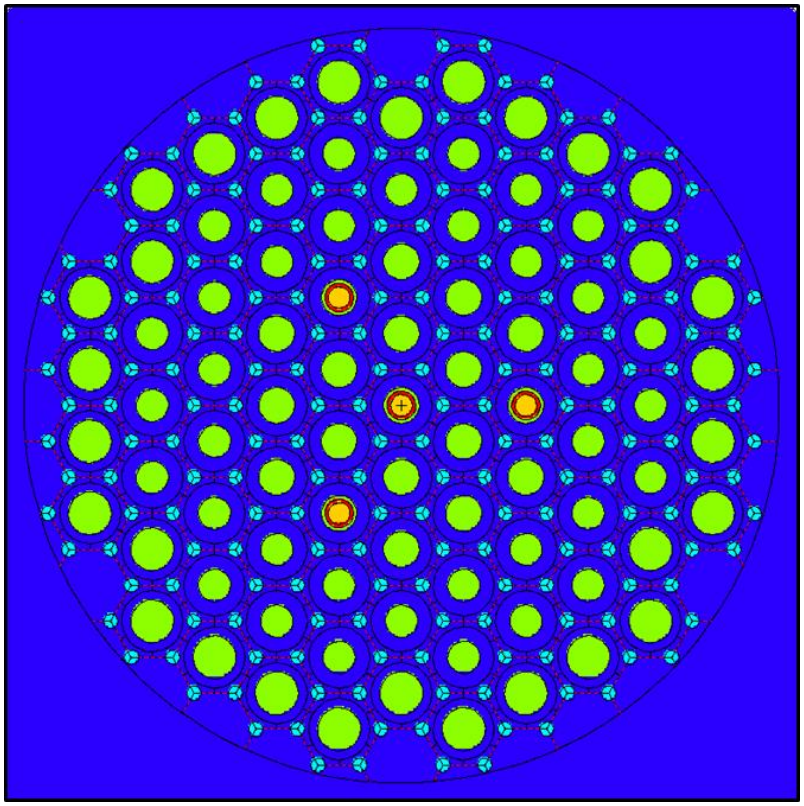

Figure 3.15. Cross Section of Final Configuration with Control Rods

3.7 BURNUP STUDY

Unfortunately, even with MCNPX, performing burnup calculations for a liquid fueled MSR is not nearly as intuitive as would be for a solid fueled reactor. Unique to this problem is the fact that a majority of the reactor's fuel is not even present in the model. Furthermore, liquid fueled reactors have the benefit of having the fuel chemically treated on relatively short time scales (often on the order of weeks) if not continually. This lack of isolation means that accurately modeling the burnup of the system will often require coupling different software and having a relatively good knowledge about the nature of the chemical processing system. Because such knowledge exceeds the scope of this thesis, various approximations will have to be made to obtain useful information.

In order to perform a burnup calculation in MCNPX, the user must first specify the total volume of the material of interest. Because the fuel will be constantly flowing throughout the system, the total volume of the fuel far exceeds the volume of the fuel present in the core. Knowing this total fuel volume requires knowing a great deal about the entirety of the primary system. Unfortunately, designing the entire primary system is impractical so the volume must be approximated. Due to the similar goals of the MSR Fuji, one can assume that the ratio of thermal power to mass of uranium 233 will be similar in magnitude. Setting the two equal to one another results in an initial loading of approximately 133 kg of uranium 233 [6]. From there the total fuel volume can be adjusted such that exactly this amount is present in the system. Doing so results in a fuel volume of approximately 4.5 cubic meters.

Using this fuel volume a series of burnup simulations were run using a single time step of 180 days and a constant power of 75 MW. Each simulation used fission products from MCNPX's Burnup Tier 2 and only varied by the omission of select fission products. Specifically, one job was run with zero omissions, one with the omission of all gaseous fission products, and one with the omission of gaseous fission products and protactinium 233. With each of these simulations, the rate of reactivity loss was calculated and used to determine the minimum refueling interval of the uranium. The results of these calculations are summarized in Table 3.4.

Table 3.4. Reactivity Loss Rates and Refueling Intervals for Burnup Models

Model	**Reactivity Loss Rate**	**Refueling Interval**
All Poisons	-0.02824 %Δk/k - day	17 days
No Gaseous Poisons	-0.01828 %Δk/k - day	30 days
No Gaseous Poisons & No Pa233	-0.01548 %Δk/k - day	45 days

Additionally, the burnup studies can offer insight on other important aspects of the reactor design. Specifically, the conversion ratio can be approximated by taking the ratio of the (n,fission) reaction rate of uranium 233 and the (n,γ) reaction rate of thorium 232. Of course, this method ignores the consumption of any protactinium 233 left within the fuel salt. Burnup studies also reveal the rate at which uranium and thorium are lost and the rate at which protactinium is created. Finally, the lifetime of the core can be determined by evaluating the magnitude of the fast (> 50 keV) flux throughout the core. Combined with the fast fluence limit of graphite (3.0E22 n / cm^2) the lifetime can be directly calculated [3]. All of these parameters are summarized in Table 3.5.

Table 3.5. Miscellaneous Reactor Burnup Parameters

Parameter	**Value**
Initial Conversion Ratio	0.97
Uranium 233 Consumption Rate	26.7 g / day
Thorium 232 Consumption Rate	77.7 g / day
Protactinium 233 Transmutation Rate	16.3 g / day
Max Fast Flux (In Core)	7.7 E13 n / cm^2 s
Max Fast Flux (In Reflector)	3.0 E13 n / cm^2 s
Max Life of Center Assembly	12.3 years
Max Life of Reflector	31.6 years

3.8 NEUTRONICS OF ALTERNATIVE FUEL CHANNEL ASSEMBLIES

Thermo hydraulic studies discussed in Section 5.2 revealed that the heat transfer surface area between the fuel and the graphite might be insufficient to make in core heat removal feasible. In an attempt to address this, alternative fuel channel assemblies were designed with the intent of maximizing the heat transfer surface area. Specifically, assemblies with a hexagonal lattice of smaller fuel channels were considered. Cross sectional diagrams of the proposed designs are shown in Figure 3.16.

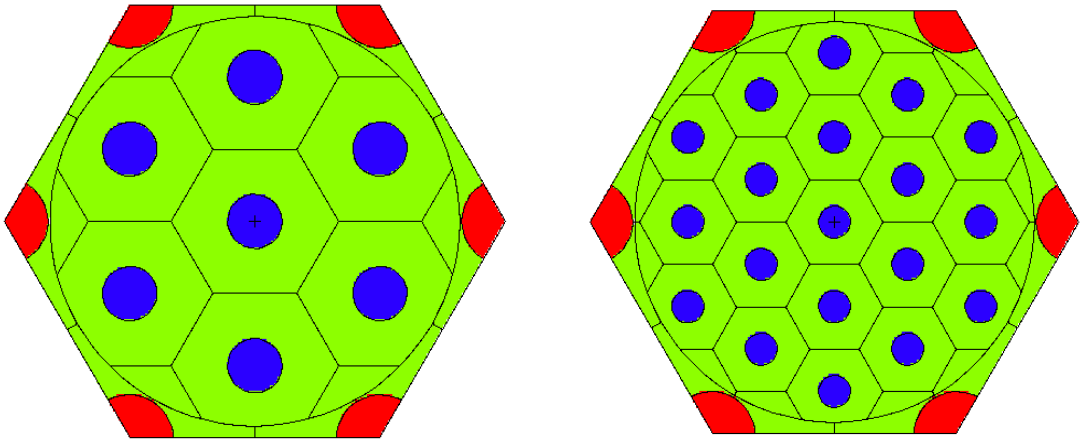

(a) Two Row Assembly (b) Three Row Assembly

Figure 3.16. Cross Sections of Alternative High Surface Area Fuel Assemblies

The alternative designs are capable of containing the same volume of fuel as the design optimized in Section 3.1, while still having a much larger heat transfer surface area. Ideally, this design would aid in the transfer of heat from the fuel to the graphite. However, the design must still be feasible from a neutronics stand point in order to be used in the final reactor design. To test this, the fuel volume fraction study performed in Section 3.1 was repeated for the two designs shown in Figure 3.16. The results of this study are shown plotted in Figure 3.17.

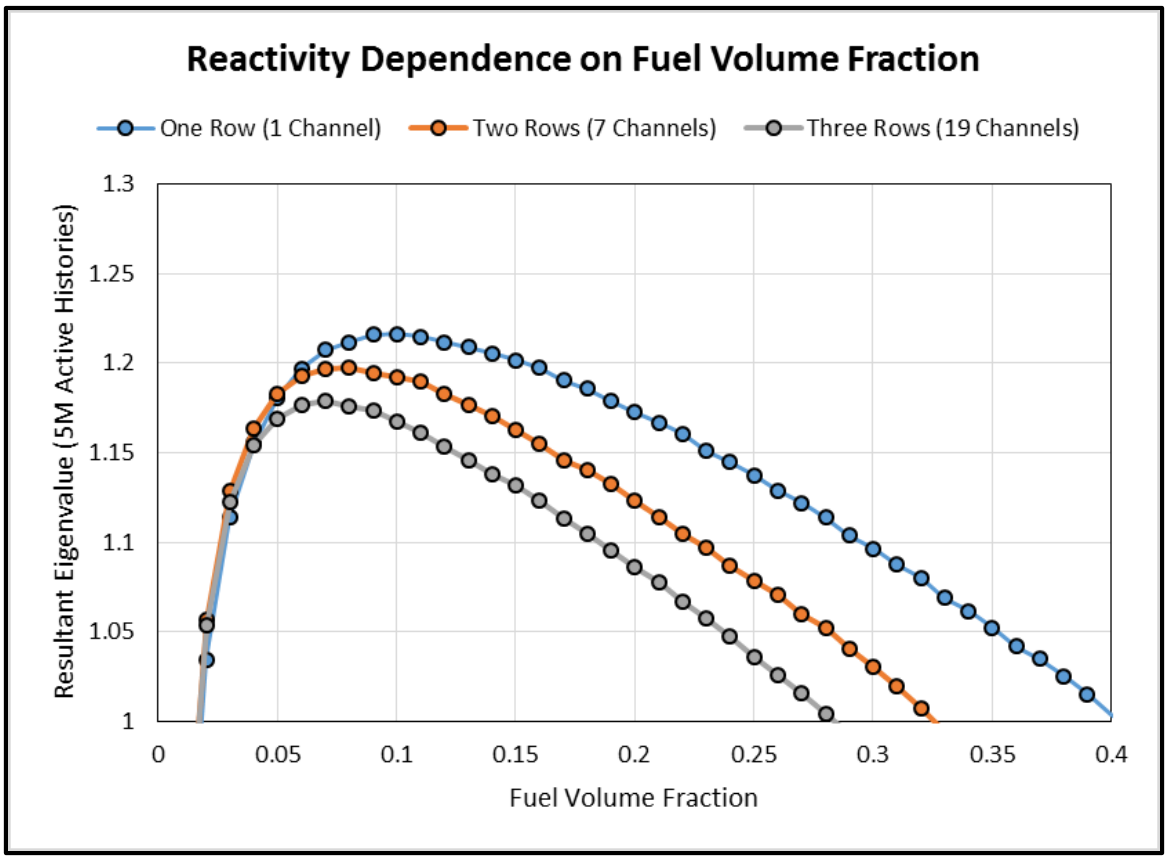

Figure 3.17. Resultant Eigenvalues of Alternative Fuel Channel Assemblies

It is clear from the results in Figure 3.17, that the original optimized fuel channel design from Section 3.1 has superior performance. However, the results also show that both of the designs are viable if the proper fuel volume fraction is implemented. These designs could, therefore, be implemented in the reactor if deemed necessary by the thermo hydraulics. It should be noted though, that a complete replacement throughout the reactor would result in a significant loss in reactivity that would need to be accounted for. Additionally, the control systems discussed in Section 3.6 would need to be reworked to accommodate the smaller fuel channels.

4. THERMO HYDRAULICS MODELING FRAMEWORK

To assess the feasibility of coupling the heat generation and heat removal processes, a series of thermo-hydraulic models were run using the CFD solver and visualizer STAR-CCM+. A model of the neutronics optimized reactor from Section 3 was created using STAR CCM+'s native CAD modeling environment. A depiction of this primary model used is shown below in Figure 4.1.

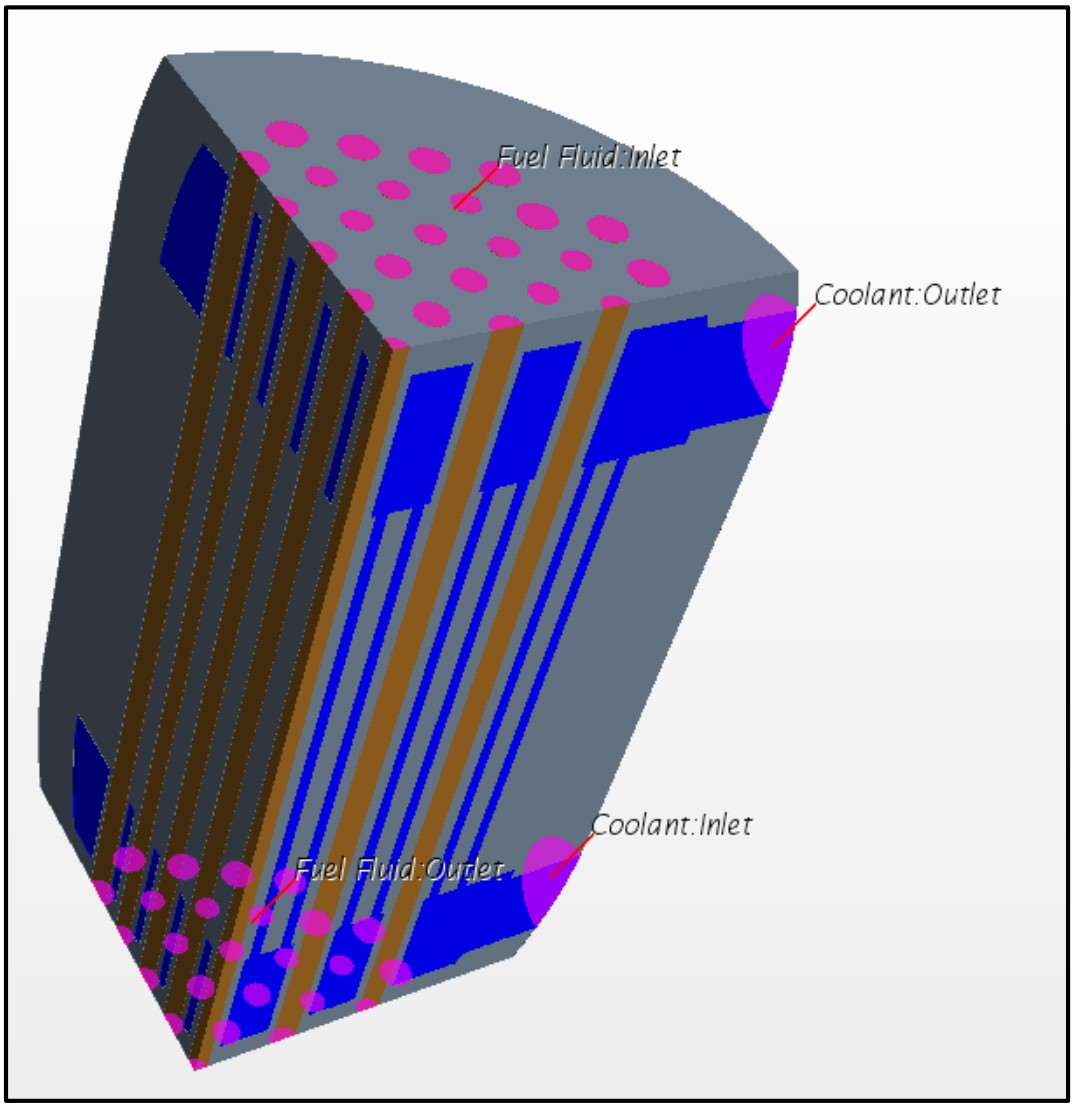

Figure 4.1. STAR-CCM+ Primary Two Fluid Reactor Model
(Coolant depicted in blue, Fuel depicted in brown, Graphite depicted in grey)

It can be quickly observed that the fuel path has no formal inlet or outlet defined in the model. This is primarily because a system to redistribute the fuel flow at the inlet of the reactor has yet to be designed. Preliminary studies quickly revealed that naïve inlet and outlet designs lead to stagnation zones where over-heating can easily occur. Unfortunately, the design of such a system exceeds the scope of this thesis and shall not be addressed within. It should be noted however, that without a formal inlet the fluid will not have the opportunity to fully develop which could result in unphysical results. This potential source of error will need to be accounted for before the design can be considered complete.

Both fluids were modeled as steady state, three dimensional, turbulent flows of constant density using the Reynolds-Averaged Navier-Stokes equations. The choice of using turbulence models was based on the range of mass flow rates tested and discussed in Section 5. Specifically, both turbulent flows were modeled using a K-Epsilon Turbulence model available within and recommended by STAR CCM+. Finally, all three regions used polyhedral meshes generated with 2 prism layers with a base size of 5 cm.

The model shown in Figure 4.1 has seven boundaries of interest: the fuel inlet, the fuel outlet, the coolant inlet, the coolant outlet, the core boundary, and the two planes of symmetry. For both the inlet boundaries, the mass flow rate and the temperature of the fluid must be specified. In contrast, no information need be specified at either of the fluid's outlets where the only restriction on the solution is mass conservation. For the core boundary, a heat flux or temperature must be specified. And finally, no information is needed for the planes of symmetry other than the fact that they are symmetric boundary conditions. Thus the user can control the solution by manipulating the mass flow rates and inlet temperatures of the two fluids as well as specify the thermal treatment at the core boundary.

Additionally, the model requires that initial conditions be specified for the three material regions as well as the volumetric heat source within the fuel. If a unique steady state solution exists, the initial conditions are arbitrary in the sense that they can only serve to speed up the convergence by being close to the final solution. By contrast, the volumetric heat source specification will fundamentally affect the final solution and must be specified as accurately as possible. Thankfully, this information can be easily obtained from MCNP5 using a F4 tally mesh with a fission cross section multiplier. Of course, the mesh data from MCNP represents flux, not power density, and must first be multiplied by a global conversion factor to convert it. That is:

$$F\langle\sigma_f\varphi\rangle_{ijk} = \langle q'''\rangle_{ijk} \quad \textbf{(2)}$$

Where:

F is some constant conversion factor

$\langle\sigma_f\varphi\rangle_{ijk}$ is the average flux – fission cross section product in mesh cell ijk as computed by MCNP

$\langle q'''\rangle_{ijk}$ is the average power density in mesh cell ijk

This correction factor can be easily calculated by noting that:

$$F\sum_{ijk}\langle\sigma_f\varphi\rangle_{ijk}V_{ijk} = P \quad \textbf{(3)}$$

Where:

V_{ijk} is the volume of mesh cell ijk

P is the total power or heat generated by the system

It is important to note that multiple regions can occupy any individual MCNP mesh cell unlike mesh cells in STAR-CCM+. Unfortunately, this contrast introduces inaccuracies in the heat source specification. Mesh cells in MCNP that contain multiple materials will generate deceptively low power density averages because of the non-fueled region's contribution (which is identically zero) to the average. For each STAR-CCM+ mesh cell, the program simply locates the closest specified MCNP mesh cell and uses its power density without interpolation. Ultimately this means that the STAR-CCM+ model will produce lower powers near region boundaries and higher powers away from them, still conserving the true total power. It is unclear how much error these inaccuracies add to the final solution, but they are thought to be less than any other method of power specification. Ideally, any significant errors can be made negligible by a sufficiently fine MCNP mesh.

5. THERMO HYDRAULICS FEASIBILITY STUDIES

As mentioned in Section 4, the user must specify the mass flow rates and inlet temperatures of the two fluids. Unless otherwise mentioned, all studies discussed will make the conservative assumption that the core boundary is adiabatic; effectively limiting all heat removal to the two fluids.

The melting temperature of approximately 732 K of Li_2BeF_4 sets a lower bound on the inlet temperature of the coolant [4]. Based on this limitation and historical data from the Molten Salt Reactor Experiment (MSRE), a conservative 800 K will serve as the coolant's inlet temperature [9]. From there, a mass flow rate can be chosen based on a desired temperature increase in the coolant. For example, a temperature rise of approximately 50 K while absorbing 75 MW will require a flow of 620 kg/s.

The fuel's temperature is limited by its boiling temperature (1800 K) and temperature limitations of the structural material Hastelloy (1400 K) [3]. For conservatism and to account for potential accident conditions the fuel's temperature shall be limited to approximately 1000 K. Ideally, the fuel should not gain or lose significant temperature while flowing through the core, so this temperature limit can also serve as the inlet temperature. This leaves only the mass flow rate of the fuel to be specified.

For an initial guess, a minimum mass flow rate can be derived by noting the simple steady state condition:

$$\int_S q'' dA = P \tag{4}$$

Where:

q'' is the local heat flux

S is the surface where heat exchange is to take place

P is the total power or heat generated by the system

Because this is primarily convective heat transfer, the heat flux can be replaced by a heat transfer coefficient and a temperature difference between the fluid and the surface. To determine the heat transfer coefficient, consider the Dittus-Bölter equation:

$$\left(\frac{hD}{k}\right) = 0.023\left(\frac{\rho v D}{\mu}\right)^{0.8}\left(\frac{\mu c_p}{k}\right)^{0.33} \quad \textbf{(5)}$$

Where:

$\left(\frac{hD}{k}\right)$ is the Nusselt number

$\left(\frac{\rho v D}{\mu}\right)$ is the Reynolds number

$\left(\frac{\mu c_p}{k}\right)$ Is the Prandt number

Combining the condition from Equation 4 with Equation 5 result in the following expression:

$$\int_S \frac{0.023k}{D}\left(\frac{\rho v D}{\mu}\right)^{0.8}\left(\frac{\mu c_p}{k}\right)^{0.33} \Delta T dA = P \quad \textbf{(6)}$$

If only the hottest channel is considered and the temperature dependence of the fluid properties are ignored, then the expression will simplify to:

$$\frac{0.023k}{D_H}\left(\frac{\rho v_H D_H}{\mu}\right)^{0.8}\left(\frac{\mu c_p}{k}\right)^{0.33}\int_{S_H} \Delta T dA = F_{xy}\left(\frac{P}{N}\right) \quad \textbf{(7)}$$

Where:

H is the index of the hottest channel

F_{xy} is the axially averaged power peaking factor

N is the total number of channels

Next, the expression can be further simplified with a crude approximation of the integral and by assuming that the mass flow rate will be uniform between channels. Doing so derives:

$$0.023k\left(\frac{4\dot{m}}{\pi N D_H \mu}\right)^{0.8}\left(\frac{\mu c_p}{k}\right)^{0.33}\pi\langle\Delta T\rangle\Delta z = F_{xy}\left(\frac{P}{N}\right) \quad \textbf{(8)}$$

Where:

$\dot{m}$ is the total mass flow rate

Δz is the axial length of the heat exchange surface

Finally, the expression can be solved for the mass flow rate to reveal:

$$\dot{m} = \frac{\pi N D_H \mu}{4}\left[\left(\frac{F_{xy}P}{0.023\,Nk\pi\,\langle\Delta T\rangle\,\Delta z}\right)\left(\frac{k}{\mu c_p}\right)^{0.33}\right]^{1.25} \quad \textbf{(9)}$$

Using the parameters shown in the following table, the initial guess for the required mass flow rate can be calculated to be approximately 2400 kg / s. It should be noted that this mass flow rate may in fact result in a Reynolds number beyond the range of applicability of Equation 7. However, because this is simply an initial guess, verification is unnecessary.

Table 5.1. Relevant Parameters for Initial Mass Flow Rate Guess

Parameter	**Value**
N	85
D_H	0.10 m
μ	0.0071 Pa - s
F_{xy}	2.2
P	75.0 MW
k	1.00 W / m – K
$\langle \Delta T \rangle$	100 K
Δz	2.0 m
c_p	1550 J / kg – K

One can quickly observe that this mass flow rate is relatively high for the power produced by the system. In fact it is the case that this mass flow rate is higher than those used in the Molten Salt Reactor Experiment (MSRE) per unit power [9]. The results of the corresponding simulation are equally as troubling, revealing that such a configuration would only remove about 15 percent of the power generated through the coolant. Regardless, more simulations were run with increasingly high fuel mass flow rates to determine the true minimum mass flow rate and are discussed in Section 5.1.

5.1 MASS FLOW RATES STUDIES

Using the model described in Section 4, a series of simulations were run with varying fuel salt mass flow rates to access the feasibility of the design. For these studies, the mass flow rate of the coolant was held fixed at the 620 kg/s derived earlier in Section 5. Of specific interest, was the amount of heat removed from the system by the coolant salt and the fuel salt. Ideally, the fuel salt should have a net energy gain of zero, depositing all of the energy generated within into the surrounding graphite before leaving the system. In this scenario, the entirety of the heat would subsequently be deposited into the coolant salt and carried out of the system. The results of these simulations are shown below in Figure 5.1.

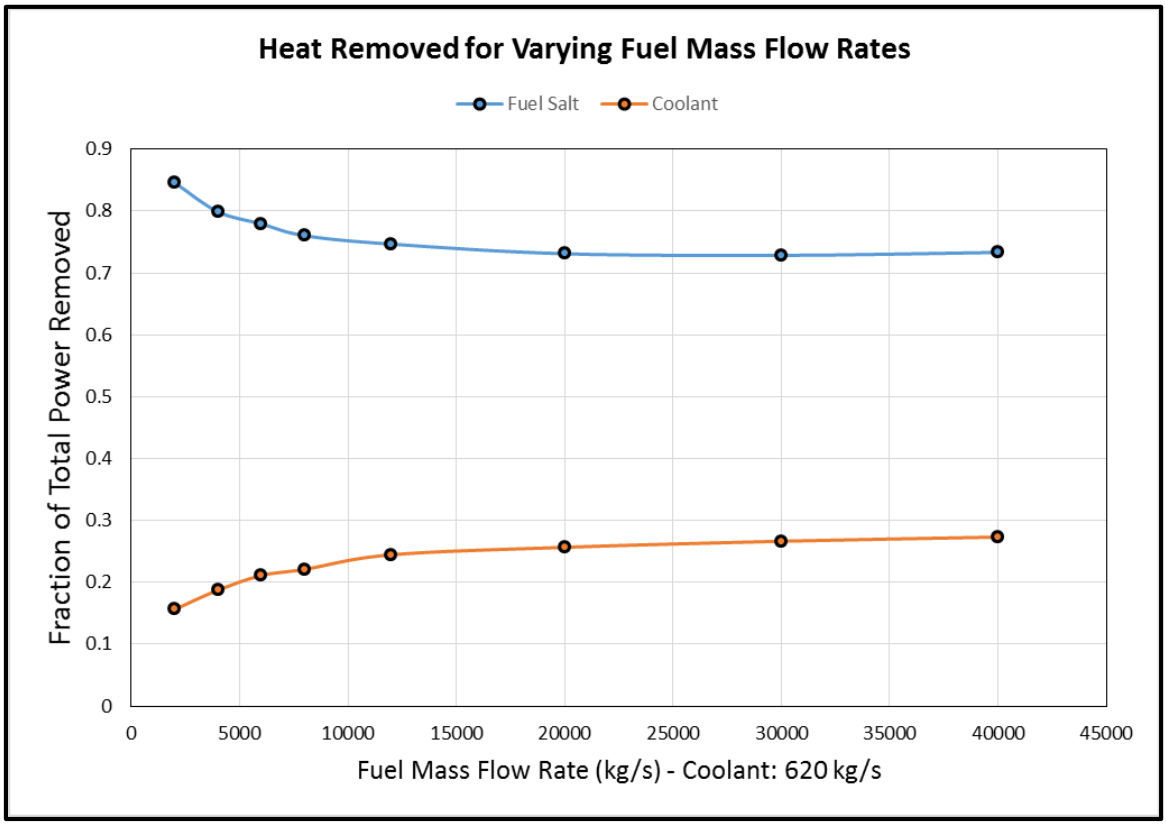

Figure 5.1. Heat Removed for Varying Fuel Mass Flow Rates

The results clearly show that even at extreme mass flow rates, the fuel cannot successfully deposit the entirety of the power generated within to the graphite walls. In fact, it appears at a certain threshold any gains in heat flux from increased fluid velocities are canceled entirely by the resultant increase in wall temperatures. Furthermore, such high fuel velocities would destroy the entire purpose of such a configuration. Despite this, more simulations were performed by instead varying the mass flow rate of the coolant. For this study the mass flow rate for the fuel was held fixed at 20,000 kg/s, the apparent location of the dimensioning returns on heat removal. The results of this study are shown in Figure 5.2.

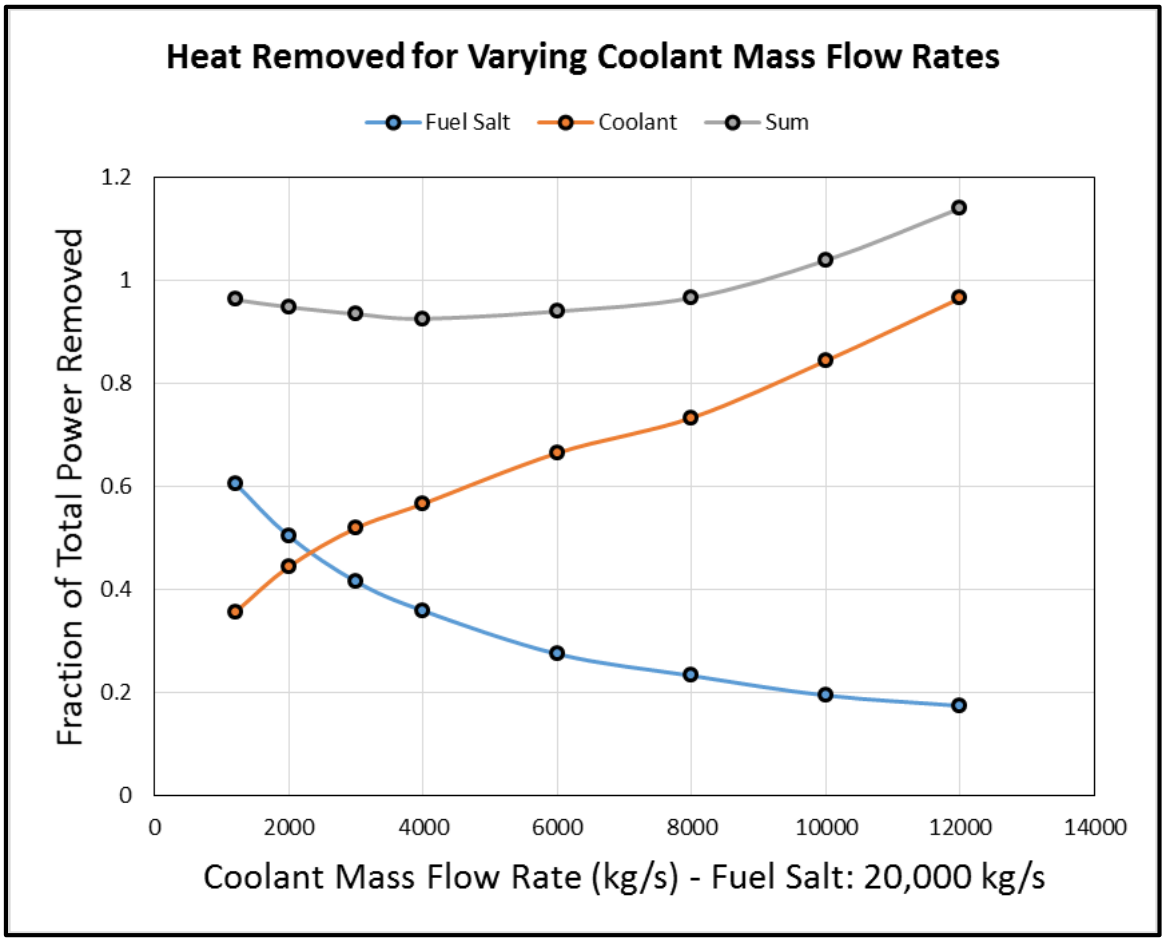

Figure 5.2. Heat Removed for Varying Coolant Mass Flow Rates

As expected, increasing the mass flow rate of the coolant results in the fuel losing a greater fraction of its generated heat. This is obviously a direct result of the coolant removing more heat from the intermediate graphite, allowing it to maintain much lower wall temperatures. Regardless, even at mass flow rates as high as 12,000 kg/s complete in core heat removal was never observed. In fact, the reliability of the convergence of solutions in these high velocity regimes becomes questionable. As seen in Figure 5.2, the sum of fractional powers removed actually begins to surpass the total power produced by the system.

6. CONCLUSIONS

The work shown within reveals that the developed design optimized for neutronics cannot feasibly support complete in core heat removal. Due to the limited surface area available to transfer heat between the fluids within the core, mass flow rates must actually increase despite the increased average temperature difference achieved by such a configuration. While it is still conceptually true that increases in the temperature difference between fuel and coolant will result in slower fuel velocities, the core would have to be designed with heat transfer surface areas on par with that of traditional heat exchangers for the effect to become apparent.

Such a reactor would likely feature unique geometries that may not be as optimized for neutronics. For example, many rectangular or elliptical channels may be beneficial for their higher surface area per unit volume. It is also possible that the loss of favorable neutronics would force an increase in the reactor's size removing it as a potential small modular reactor. Further work would have to be done on such a design if the proposed advantages are desirable.

It should be noted that the reactor design developed within is still neutronically feasible despite not meeting the goal of complete in core heat removal. A simple traditional external heat exchanger is the only addition needed to ensure that the design would be functional. One can even imagine a scenario where the design operates in steady state with a fraction of its heat being removed directly from the core (with the rest being removed by traditional means). Without further analysis, it is unclear how beneficial such a configuration would be but even fractional in core heat removal would serve to increase the average temperature of the fuel throughout the system. Further, by simply removing the developed

coolant channels and accounting for any increases in reactivity the developed design still serves as an excellent starting point for a traditional small modular MSR.

The two fluid small modular molten salt reactor has been optimized in favor of minimal physical size and a variety of neutronics concerns. The core and reflector have a total combined diameter of approximately 2.9 meters leaving a total 35 centimeter thickness for piping and shielding components surrounding the core. It should be noted that all studies were performed assuming any neutrons that leave the graphite reflector will not reflect back into the core. Realistically, this will not be the case and the reflector size may be slightly reduced to compensate for any increase in reactivity observed from further model refinement. It is thought that at this size the reactor core, its primary piping components, pumps, and primary heat exchangers can all be fit within the 3.5 meter diameter rail shipping restrictions. However it should be noted that, as built, the reactor will not be sufficiently shielded which will have to be accounted for on-site.

With this design, the reactor would operate safely at a thermal power of 75 MW for 10 years without changing any of the graphite components. If replacing the graphite channels every 10 full power years is considered viable, the reactor will run for 30 full power years before the integrity of the reflector becomes compromised. At this point, the reactor fuel can be drained from the core to be used in another reactor and the graphite will be handled as radioactive waste. Additionally, because the fuel can be reprocessed online, the reactor has the capability to run the entire 10 year intervals uninterrupted.

During stable operations, the reactor will operate with essentially no excess reactivity making the event of a power transient unlikely. Should an accident still occur, the reactor has a variety of ways to shut itself down. The four control rods offer enough reactivity to ensure

shutdown during any operational state with one-stuck rod condition. Additionally, the increase in temperature that would result from a power transient would immediately result in a negative reactivity insertion due to the large negative temperature reactivity coefficient of the fuel. Should all else fail, the temperature increase in the fuel would inevitably melt the freeze plug required to keep the fuel in the core without any human intervention. This would force the fuel to safely drain from the core into the subcritical storage tanks located below.

BIBLIOGRAPHY

[1] D. LeBlanc, "Molten salt reactors: A new beginning for an old idea," Nucl. Eng. Des. , 2010.

[2] R. C. Briant and A. M. Weinberg, "Molten Fluorides as Power Reactor Fuels," vol. 2, 1957.

[3] "Status of Small Reactor Designs Without On-Site Refuelling," IAEA, Vienna, Austria, 2007.

[4] D. T. Ingersoll, E. J. Parma and C. W. Forsberg, "Core Physics Characteristics And Issues For The Advanced High - Temperature Reactor (AHTR)," Oak Ridge National Laboratory & Sandia National Laboratory.

[5] B. J. Marsden, "Nuclear Graphite for High temperature Reactors," AEA Technology, Risley, Warrington .

[6] "MSR-FUJI General Information, Technical Features, and Operating Characteristics".

[7] C. R. Robertson, O. L. Smith, R. B. Briggs and E. S. Bettis, "Two-Fluid Molten Salt Breeder Reactor Design Study (Status as of January 1, 1968)," Oak Ridge National Laboratory, Oak Ridge, Tennessee, 1970.

[8] E. S. Bettis, L. G. Alexander and H. L. Watts, "Design Studies of a Molten-Salt Reactor Demonstration Plant," Oak Ridge National Laboratory, Oak Ridge, 1972.

[9] P. N. Haubenreich, J. R. Engel, B. E. Prince and H. C. Claiborne, "MSRE Design And Operations Report Part III Nuclear Analysis," Oak Ridge National Laboratory, Oak Ridge, Tennessee, 1964.

VITA

Brandon James Lahmann was born in St. Louis, Missouri on August 15, 1990. He received his Bachelors of Science in Nuclear Engineering with Honors Fellow and Summa Cum Laude distinctions from the Missouri University of Science and Technology in May 2013. During his undergraduate career, Brandon was actively involved in the university's local chapters of Alpha Nu Sigma, the American Nuclear Society, and Women in Nuclear. Additionally, he worked for the university as a Peer Learning Assistant, helping fellow students in subjects such as differential equations, thermodynamics, and electrical circuit analysis. Brandon is near the completion of his Masters of Science in Nuclear Engineering from the same university which he plans to obtain in May 2014. Upon completing his Masters, Brandon will go on to Massachusetts Institute of Technology to begin work on his Doctor of Science in Nuclear Science and Engineering.

In November of 2011, Brandon earned his Senior Reactor Operator's License at the Missouri University of Science and Technology Reactor which he has managed to maintain to this date. In the summer of 2012, he interned for Knolls Atomic Power Laboratory (KAPL) where he established the first official user design procedure for the Monte Carlo code MC21. Brandon returned as in intern to KAPL in the summer of 2013 where he designed and developed an automated reactor geometry generator in Java for the laboratory's physics community. Starting in the summer of 2014, Brandon intends to work for Sandia National Laboratories where he will work to upgrade and modify a Monte Carlo DD and DT fusion reaction product code.